Magnetic anisotropy of pure and doped $YbInCu_4$ compounds at ambient and high pressures

2003 J. Phys.: Condens. Matter 15 2811

(http://iopscience.iop.org/0953-8984/15/17/330)

INSTITUTE OF PHYSICS PUBLISHING JOURNAL OF PHYSICS: CONDENSED MATTER

J. Phys.: Condens. Matter **15** (2003) 2811–2823 PII: S0953-8984(03)59274-8

Magnetic anisotropy of pure and doped $YbInCu_4$ compounds at ambient and high pressures

N V Mushnikov[1,2,4], T Goto[1], E V Rozenfeld[2], K Yoshimura[3], W Zhang[3], M Yamada[1] and H Kageyama[1]

[1] Institute for Solid State Physics, University of Tokyo, 5-1-5 Kashiwanoha, Kashiwa, Chiba 277-8581, Japan
[2] Institute of Metal Physics, Kovalevskaya 18, 620219 Ekaterinburg, Russia
[3] Department of Chemistry, Graduate School of Science, Kyoto University, Kyoto 606-8502, Japan

E-mail: mushnikov@imp.uran.ru

Received 5 February 2003
Published 22 April 2003
Online at stacks.iop.org/JPhysCM/15/2811

Abstract

The susceptibility and high-field magnetization of single-crystalline $Yb_{1-x}Y_xInCu_4$ ($x = 0$, 0.2 and 0.3) samples have been measured for different field orientations at ambient and high pressures. The compounds with $x = 0$ and 0.2 undergo a first-order valence transition from the intermediate-valence state to the trivalent state on increasing either temperature or magnetic field. The magnetization and susceptibility of these compounds have appreciable anisotropy in both states. The magnetic phase diagram of $Yb_{1-x}Y_xInCu_4$ determined at ambient pressure is also anisotropic, which is explained by the crystal-field calculations for the free Yb ion in the high-temperature phase. Moreover, the low-temperature magnetization process for $x = 0.2$ and 0.3 has been measured in low fields under high pressure; it shows anisotropic ferromagnetic ordering.

1. Introduction

Ytterbium compounds display a variety of magnetic transitions because of the instability of f^{13} electronic configuration of Yb^{3+}. Since the energy states of the trivalent f^{13} and divalent f^{14} configurations are very close, a mixed-valence state is frequently realized in Yb-based compounds [1]. A small change produced in the local environment around the Yb ion will modify its electronic state and the physical properties of the compounds.

The $YbInCu_4$ compound has the cubic C15b-type crystal structure and undergoes a first-order temperature-induced isostructural valence phase transition at ambient pressure [2, 3]. Above the critical temperature $T_v \sim 40$ K the Yb ion is trivalent and the compound exhibits a

[4] Address for correspondence: Institute of Metal Physics, Kovalevskaya Street 18, 620219 Ekaterinburg, Russia.

Curie–Weiss susceptibility. The valence of the Yb ion decreases suddenly by ~ 0.1 at T_v; this accompanies a lattice constant increase of 0.15% [4–6]. In spite of the small change in the valence, both the susceptibility and the electrical resistivity decrease substantially and a Pauli-paramagnetic (Fermi-liquid) state is realized below T_v. The application of a high magnetic field destabilizes the mixed-valence state: a metamagnetic-like field-induced valence transition to the trivalent state is observed at a critical field B_v [7, 8].

The valence transition of $YbInCu_4$ is easily affected by either applying high pressure or alloying. The pressure effect on the critical temperature T_v was studied by means of resistivity, magnetic susceptibility and thermal expansion measurements [2, 3, 9, 10]. The value of T_v is found to decrease on applying pressure; $\mathrm{d}T_v/\mathrm{d}P \sim -20$ K GPa^{-1}. This is consistent with the stabilization of the high-temperature trivalent state of Yb having smaller size. The pressure effect on the critical field B_v is reported to also be negative; $\mathrm{d}B_v/\mathrm{d}P \sim -10$ T GPa^{-1} [11]. With proper alloying on the Yb or the In site, on the other hand, both the critical temperature and field are increased or decreased simultaneously [3, 4, 12]. In the case of substitution of Y for Yb, the valence transition shifts to the low-temperature low-field region [3, 11–13]. Although the mixed-valence state of the parent $YbInCu_4$ survives even at 2.5 GPa [14], that of $Yb_{0.8}Y_{0.2}InCu_4$ disappears under high pressure of above 1 GPa and the trivalent state exists over the entire temperature range [11]. It should be noted that a weakly ferromagnetic state with a magnetic moment of 0.05 μ_B/Yb appears below 1.7 K at 1.2 GPa [15].

The formation of the low-temperature Fermi-liquid state in $YbInCu_4$ derives from the interaction between f electrons of Yb in the mixed-valence state and conduction-band electrons [16]. As a first approach, the Anderson single-impurity model is applied to clarify the low-temperature behaviour of a periodic lattice of magnetic Yb ions [1]. The Bethe ansatz solution to the Coqblin–Schrieffer model (the Anderson single-impurity Hamiltonian in the Kondo limit) describes quantitatively the physical properties of some Yb compounds having a continuous valence transition with temperature [1, 17, 18]. In order to explain the first-order transition in $YbInCu_4$ within the framework of the Anderson model, the electron–lattice coupling and the Coulomb repulsion between the f- and conduction-band electrons were taken into account [16]. Since this model does not include the interaction of the f electrons with the crystal electric field, the magnetic behaviour deduced is completely isotropic. On the other hand, the importance of anisotropic interactions in the magnetism of Kondo systems has been pointed out [19–21]. The $J = 7/2$ ground state multiplet of an Yb^{3+} ion in a cubic crystal field is split into a Γ_6 doublet, a Γ_7 doublet and a Γ_8 quartet [22]. The splitting causes anisotropy of the paramagnetic susceptibility. However, the effect of the crystal electric field on the high-temperature susceptibility is expected to be very small since the splitting is modest (total splitting $\Delta = 44$ K [23]). In the Coqblin–Schrieffer model the crystal field results in the occurrence of anisotropic coupling between conduction and 4f electrons at low temperatures [24]. Recently, the magnetic phase diagram of $YbInCu_4$ was studied theoretically, considering crystal-field effects [25]. It was shown that the calculated phase diagram in the B–T plane has some anisotropy with respect to the direction of an external magnetic field applied to the cubic lattice.

The valence transition in $YbInCu_4$ is extremely sensitive to small variation in the stoichiometry and site disorder [26]. Therefore, many of the studies were performed using single-crystalline samples, which, as a rule, were more homogeneous and showed a sharper transition than polycrystals [3, 11]. However, the orientation of the samples was not determined, since the anisotropy of the physical properties was expected to be very small. In the present study we have measured the magnetic susceptibility and the high-field magnetization curve of $Yb_{1-x}Y_xInCu_4$ with $x = 0$, 0.2 and 0.3 at ambient and high pressures using oriented single crystals to examine the crystal-field effects in the magnetization and field-induced

valence transition. Moreover, we have carefully measured the low-field magnetization process of $Yb_{1-x}Y_xInCu_4$ with $x = 0.2$ and 0.3 under high pressure to study the anisotropy of the ferromagnetic ordering found by Mitsuda *et al* [15].

2. Experimental details

Single crystals of pure and substituted $YbInCu_4$ compounds were grown from an In–Cu flux [26, 27]. Polycrystalline samples were first prepared by arc-melting of the starting elements mixed in a one-to-one ratio of $Yb_{1-x}Y_xInCu_4$ to $InCu_2$ in an argon atmosphere. The ingot was crushed into a powder, placed in an alumina crucible and then sealed in an evacuated quartz tube. Subsequently the powder sample was heated to 1000 °C and cooled very slowly to 800 °C, at which point the flux was separated from single crystals. Single-crystalline samples were oriented using an x-ray Laue diffractometer with a Polaroid camera. Two parallel faces were ground perpendicular to each of the [001], [1$\bar{1}$0] and [111] axes of the cubic crystals. The oriented samples have the shape of a right-angle prism with a volume of $\sim$2.5 mm^3. Hereafter we denote the principal axes as [100], [110] and [111], respectively.

The magnetic susceptibility was measured using a Quantum Design SQUID magnetometer at ambient pressure in the temperature range 5–200 K in a magnetic field 0.5 T. The magnetization under pressure was measured with an extraction-type magnetometer in magnetic fields up to 9 T produced by a superconducting magnet. Hydrostatic high pressure was applied to the sample up to 1.3 GPa using a non-magnetic clamp pressure cell made of a CuTi alloy. The oriented sample inside the cell was placed in a Teflon capsule filled with a liquid pressure medium, Fluorinert. A He^3 cryostat was used to cool the sample together with the pressure cell down to 0.6 K. The details of the measurement system are described in [28]. The high-field magnetization curve was measured by an induction method in pulsed magnetic fields up to 42 T with a pulse duration time of $\sim$20 ms. The shape of the magnetization curve for bulk single crystals coincides with that for powdered samples of the same compositions, ensuring that the eddy current effect is negligibly small. The uncertainties in the absolute value of the field and magnetization are 0.5 and 2%, respectively, while the uncertainties due to the change of the sample orientation are $\pm$0.1 T and $\pm$0.02 μ_B/Yb.

3. Experimental results

The magnetic susceptibility of $YbInCu_4$ has been measured previously by many researchers (see, e.g., [3]). For homogeneous samples, two temperature ranges of distinct behaviour were observed. Above the temperature of the valence transition T_v, the susceptibility obeys a Curie–Weiss behaviour with a very small negative paramagnetic Curie temperature θ. Below T_v the sample is characterized by considerably lower Pauli-paramagnetic susceptibility, which is nearly temperature independent. Figure 1(a) shows the temperature dependence of the magnetic susceptibility χ of a $YbInCu_4$ single crystal measured with a SQUID magnetometer in a magnetic field of 0.5 T applied along main crystallographic directions with increasing temperature. The single crystal exhibits a very sharp valence transition at $T_v = 43$ K. Although the transition temperature does not depend on the direction of the applied magnetic field, the values of the susceptibility along the three axes are slightly different. As clearly seen from the inset in figure 1(a), the susceptibility in the low-temperature mixed-valence state is largest for the [100] axis and smallest for the [110] axis. In the case of the high-temperature trivalent state, the difference is somewhat smaller, but the same tendency is observed.

The temperature dependence of the inverse susceptibility $\chi^{-1}(T)$ shown in figure 1(b) is almost linear above T_v. The observed differences in the slope of $\chi^{-1}(T)$ for different directions

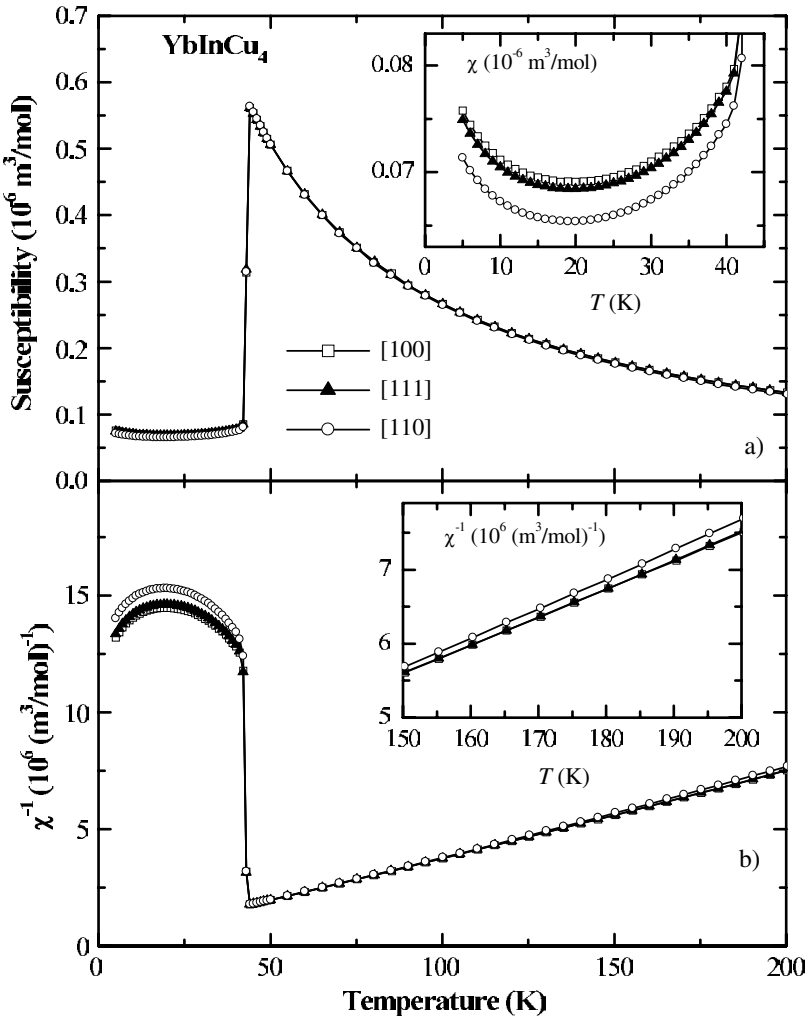

Figure 1. Temperature dependences of the molar susceptibility (a) and inverse molar susceptibility (b) of single-crystal $YbInCu_4$ measured for different crystallographic directions. The insets show two parts of the curves on a larger scale.

imply that both the paramagnetic Curie temperature θ and the effective magnetic moment μ_{eff} are anisotropic. Since the linear fits of the $\chi^{-1}(T)$ dependence for different temperature ranges give slightly different slopes, the absolute values of θ and μ_{eff} are determined with the accuracy ± 0.5 K and $\pm 0.1\ \mu_B$/Yb, respectively. At the same time, the uncertainties in the relative changes of the parameters with the sample orientation are estimated to be ± 0.02 K and $\pm 0.01\ \mu_B$/Yb. The values of θ and μ_{eff} determined from the linear fit of $\chi^{-1}(T)$ in the temperature range 50–200 K are listed in table 1. The difference between the paramagnetic Curie temperatures for the [100] and [110] directions amounts to ~ 2 K, which is quite large for cubic samples. The values of μ_{eff} determined in the present study are found to be slightly lower than the free Yb^{3+} ion value $4.54\ \mu_B$. Observation of a slightly lower value of μ_{eff} was also reported in [7, 27]. One of the possible reasons for this is the crystal-electric-field effect. The susceptibility of 4f ions is usually affected by the crystal field. Another reason is

Table 1. Summary of the magnetic parameters of $YbInCu_4$ for different field orientations.

Field orientations	[100]	[110]	[111]
Measured B_v for 4.2 K (T)[a]	32.9	34.3	33.1
Calculated B_v for 5 K (T)	31.3	34.0	32.9
Measured M for 4.2 K and 40 T (μ_B/Yb)	3.35	3.21	3.30
Calculated M for 8 K and 40 T (μ_B/Yb)	3.91	3.78	3.86
Estimated θ (K)	−2.05	−0.05	−1.91
Estimated μ_{eff} (μ_B/Yb)	4.15	4.09	4.15

[a] Averaged for field-up and field-down branches of the magnetization curve.

the deviation of the valence of the Yb ion in the high-temperature state from 3+. According to L_{III} x-ray absorption spectroscopy, the valence of Yb above T_v is estimated to be 2.93 [18] or 2.9 [4]. If the estimated value is correct, however, the high-temperature phase is also a mixed-valence state and the susceptibility is modified considerably by valence fluctuations. We believe that the valence of the Yb ion is 3+ in the high-temperature state. In terms of the Kondo impurity model, the reduction of μ_{eff} is caused by the Kondo interaction.

According to the isotropic models of the valence transition in $YbInCu_4$, there are two characteristic energy scales [16]. In the high-temperature phase $T > T_v$, the localized f electrons of Yb interact weakly with the conduction-band electrons. The thermodynamic properties of this state are described with the Kondo temperature $T_K \sim 25$ K [27]. The value of T_K can be estimated by fitting the effective moment determined experimentally to the prediction of the $J = 7/2$ Kondo model. In the low-temperature phase $T < T_v$, a Fermi-liquid state is realized, in which the f- and conduction-band states are strongly hybridized. A different Kondo energy scale T_0 determines the low-temperature thermodynamic properties. The zero-temperature susceptibility $\chi(0)$ is proportional to $1/T_0$ [17, 29]:

$$\chi(0) = \frac{N_A \nu(\nu^2 - 1) g_J^2 \mu_B^2}{24\pi k_B T_0}, \tag{1}$$

where N_A is the Avogadro number, $\nu = 2J + 1$ is the degeneracy of the ground state, g_J is the Landé factor. For $YbInCu_4$, the T_0-value amounts to 430–540 K [11, 27]. The difference between the T_0-values determined from the present susceptibility data for different axes does not exceed 7%. Hence, isotropic models are not so bad for describing the valence transition in $YbInCu_4$.

Figure 2 shows the high-field magnetization curves measured at 4.2 K along different directions of single-crystalline $YbInCu_4$. The magnetization curve for each direction indicates a sharp valence transition with hysteresis above 30 T. The magnetization M for the [110] direction is smallest in both the low- and high-field states, while the critical field is highest. The critical field B_v was attributed to the field of a maximum of the derivative dM/dB. The average value of the critical fields was determined from the field-up and field-down branches of the magnetization curve, as listed for the three principal axes in table 1. The observed anisotropy of B_v is in agreement with the magnetic phase diagram recently calculated by Dzero [25] on the basis of a simple assumption that the free energy of the low-temperature state is a constant, by taking into account crystal-field effects for the free Yb ion. According to the calculation [25], anisotropies of B_v and M exist, although anisotropy of T_v is absent in a weak field. The value of B_v at low temperatures is largest for the [110] direction and the anisotropy of B_v is of the order of 2 T. These results are consistent with our experimental values of B_v at 4.2 K. However, the calculations indicate that B_v and the magnetization M for the [100] direction have an intermediate value. (The values of B_v and M for the [111] direction are smallest and largest, respectively.) These results are inconsistent with the experimental data.

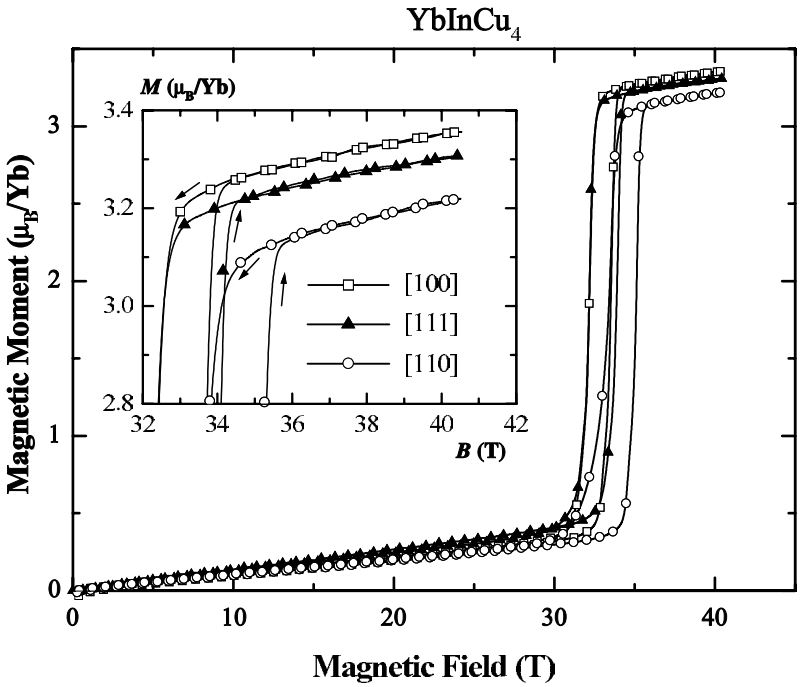

Figure 2. High-field magnetization curves of $YbInCu_4$ measured for different crystallographic axes at 4.2 K. Inset: a part of the curve on a larger scale. Arrows indicate the field sequence.

At high temperatures above T_v the anisotropy of M becomes very small. The high-field magnetization curves measured at 50 K along the three principal directions coincide within the accuracy of our high-field magnetometer.

Since the anisotropy of the magnetization curves increases with decreasing temperature, we also studied two Y-substituted single crystals, where the valence transitions are shifted to the low-temperature region. The substitution of non-magnetic Y, La and Lu for magnetic rare-earth atoms weakly affects the crystal electric field and, as a rule, does not change the type of the magnetic anisotropy. Figure 3 shows the temperature dependence of the susceptibility of single-crystalline $Yb_{0.8}Y_{0.2}InCu_4$ and $Yb_{0.7}Y_{0.3}InCu_4$ measured at ambient and high pressures in a magnetic field of 0.5 T. The critical temperature of the valence transition in $Yb_{0.8}Y_{0.2}InCu_4$ is $T_v \sim 21$ K. Zhang *et al* [11] found that the critical temperature of $Yb_{0.8}Y_{0.2}InCu_4$ is decreased together with the critical field by applying pressure and the mixed-valence state completely disappears at 1.3 GPa. On the other hand, the present $Yb_{0.7}Y_{0.3}InCu_4$ sample retains the trivalent state down to 0.6 K even at ambient pressure. The magnitude of the susceptibility in the trivalent state of the two compounds at ambient pressure is largest for the [100] direction and smallest for the [110] direction, although the difference is very small (open symbols in figure 3(b)). This indicates that the substituted compounds at ambient pressure show qualitatively the same anisotropy as the parent $YbInCu_4$.

We found that external hydrostatic pressure produces completely different effects on the anisotropy of the magnetic susceptibility for the two Y-substituted compounds. The anisotropy of $Yb_{0.8}Y_{0.2}InCu_4$ is enhanced by applying a high pressure of 1.0 GPa, but the type of the anisotropy remains unchanged (closed symbols in figure 3(a)). In the case of $Yb_{0.7}Y_{0.3}InCu_4$, an external pressure of 1.2 GPa enhances the susceptibility along the [111] direction and

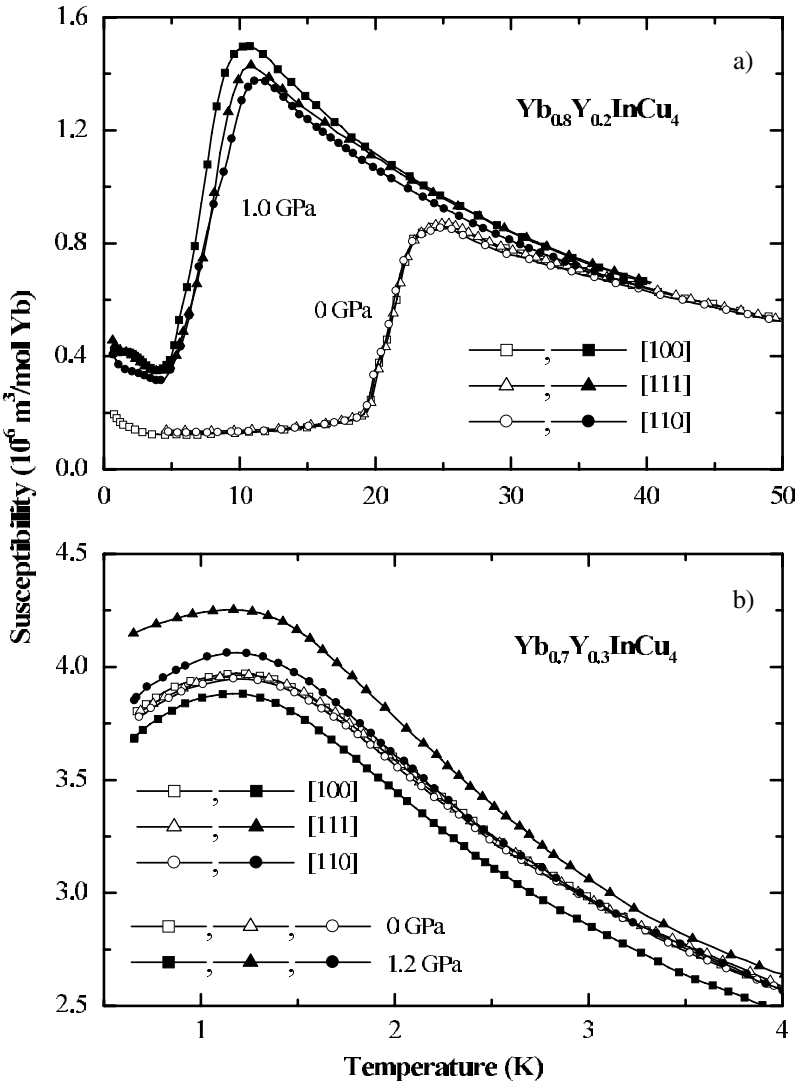

Figure 3. Temperature dependences of the molar susceptibility of $Yb_{0.8}Y_{0.2}InCu_4$ (a) and $Yb_{0.7}Y_{0.3}InCu_4$ (b) single crystals measured along different crystallographic axes for ambient pressure (open symbols) and for 1.2 GPa (closed symbols).

suppresses that along the [100] direction (closed symbols in figure 3(b)). However, this is valid only for a low-field region.

Figure 4 shows the magnetization curves of the two Y-substituted compounds $Yb_{0.8}Y_{0.2}InCu_4$ and $Yb_{0.7}Y_{0.3}InCu_4$ for 0.6 K under a high pressure of 1.0 or 1.2 GPa in steady magnetic fields up to 9 T. The first-order field-induced valence transition is considerably broadened for $Yb_{0.8}Y_{0.2}InCu_4$ in comparison with that for the pure $YbInCu_4$ compound. Perhaps the broadening comes from inhomogeneous distribution of the substituent. Y-substituted $YbInCu_4$ samples always show a broadened valence transition [11–13]. In the high-field region above 5 T, the magnitude of M, for both compounds, is largest for the [100] direction and smallest for the [110] direction, in agreement with the anisotropy of the

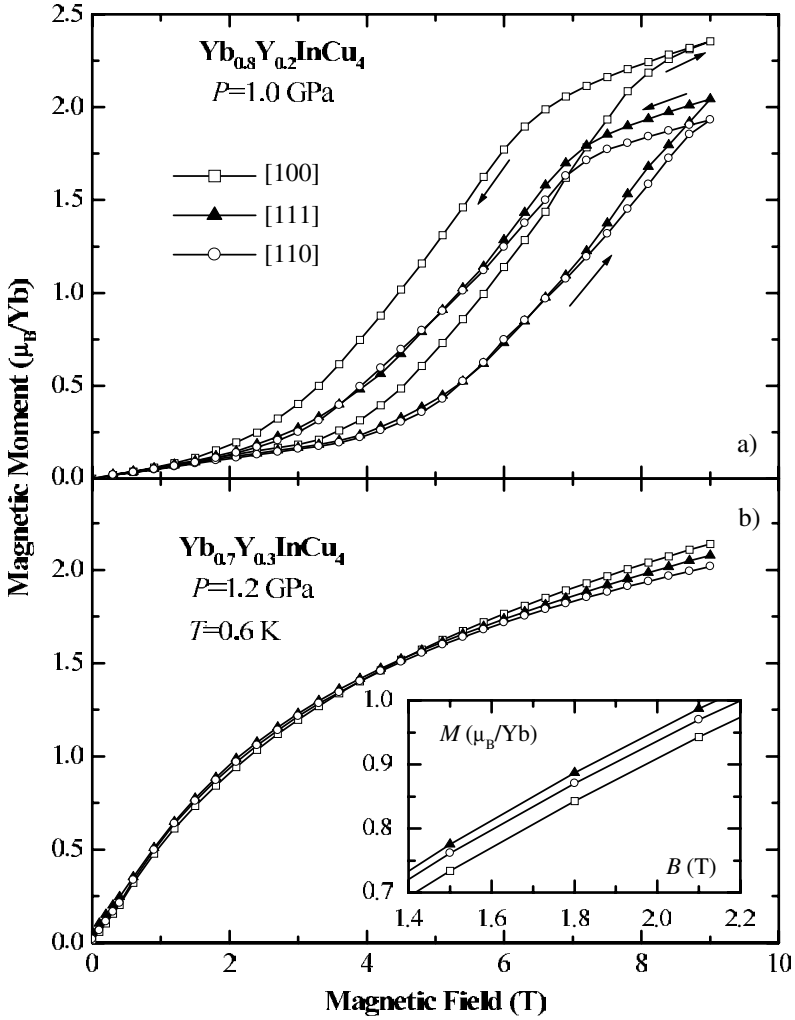

Figure 4. Magnetization curves of $Yb_{0.8}Y_{0.2}InCu_4$ for 1 GPa (a) and $Yb_{0.7}Y_{0.3}InCu_4$ for 1.2 GPa (b) measured along different crystallographic axes at 0.6 K. Inset: a part of the curve on a larger scale.

susceptibility measured at ambient pressure (figure 3(a)). It is clear also that the anisotropy of B_v of the order of 1 T persists in $Yb_{0.8}Y_{0.2}InCu_4$ under high pressure (see also figure 2).

The magnetization curves of $Yb_{0.7}Y_{0.3}InCu_4$ at 0.6 K are typical of paramagnets both at ambient pressure (not shown) and at 1.2 GPa (figure 4(b)). However, they are quite different from the simple paramagnetic magnetization curve for free Yb^{3+} ions, which is given by the Brillouin function with $J = 7/2$. This function indicates that the magnetization easily saturates to 4 μ_B/Yb ion in a magnetic field of ∼3–4 T for such a very low temperature. Thus, both the Kondo interaction and the crystal-field effect should be considered together with the RKKY interaction to explain the magnetization curve of $Yb_{0.7}Y_{0.3}InCu_4$ at low temperatures.

The observed anisotropy of the magnetization of $Yb_{0.7}Y_{0.3}InCu_4$ under pressure in high magnetic fields above 5 T is qualitatively the same as that of the other samples studied: the magnetization is largest for the [100] direction and smallest for the [110] direction. In magnetic fields below 5 T the situation changes: the magnetization of $Yb_{0.7}Y_{0.3}InCu_4$

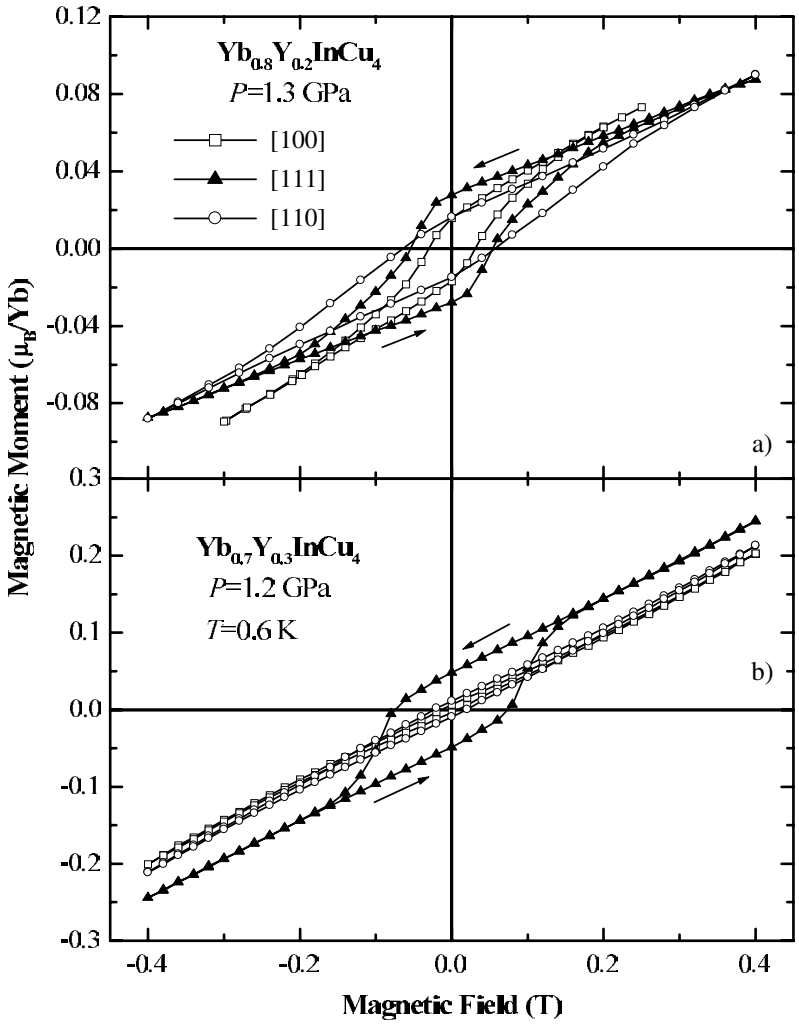

Figure 5. Low-field hysteresis loops of $Yb_{0.8}Y_{0.2}InCu_4$ for 1.3 GPa (a) and $Yb_{0.7}Y_{0.3}InCu_4$ for 1.2 GPa (b) measured along different crystallographic axes at 0.6 K.

becomes largest along the [111] direction, while it is smallest along the [100] direction (see the inset in figure 4(b)).

The paramagnetic Curie temperature θ of $YbInCu_4$ is negative as shown in table 1. This indicates that the interaction between Yb^{3+} ions is antiferromagnetic. Svechkarev *et al* [30] found that the pressure derivative $d\theta/dP$ is positive. They estimated a latent interaction in $YbInCu_4$ by plotting the value of θ against the de Gennes factor for a series of heavy rare-earth $RInCu_4$ compounds. The estimated interaction is positive. They expected that a ferromagnetic ordering might appear after the disappearance of the mixed-valence state under high pressure due to the latent positive interaction. Recently, a weakly ferromagnetic ordering was found in a single-crystalline sample of $Yb_{0.8}Y_{0.2}InCu_4$ under high pressure, $P \geqslant 0.8$ GPa [15]. Figure 5 shows the low-temperature magnetization processes of $Yb_{0.8}Y_{0.2}InCu_4$ for 1.3 GPa and $Yb_{0.7}Y_{0.3}InCu_4$ for 1.2 GPa. In the $Yb_{0.8}Y_{0.2}InCu_4$ sample, weak ferromagnetism is absent up to 1 GPa, but is clearly seen at 1.3 GPa, where the low-temperature mixed-valence state is completely suppressed. The weak ferromagnetic states for the two compounds have

appreciable magnetic anisotropy. The remnant magnetization is largest for the [111] direction, while the coercivity is smallest for the [100] direction. The hysteresis loop becomes smaller with increasing temperature. For $Yb_{0.8}Y_{0.2}InCu_4$ at 1.3 GPa the hysteresis disappears at 2.4 K simultaneously for all of the directions and the magnetization is almost proportional to the magnetic field. $Yb_{0.7}Y_{0.3}InCu_4$ at 1.2 GPa has a lower Curie temperature: the hysteresis has already completely disappeared at 1.8 K.

4. Discussion

The origin of the observed magnetic anisotropy of $YbInCu_4$ is the interaction of the anisotropic 4f orbitals of Yb^{3+} ions with the crystal electric field produced by the surrounding ions of the cubic lattice. We calculate theoretically the critical field of the valence transition and the magnetization curve for different directions of the cubic cell, taking an approach similar to that in [25].

The transition line of the magnetic phase diagram in the B–T plane can be determined from the condition that the free energies F_L and F_H of low-temperature and high-temperature phases are equal to each other:

$$F_L(T, B) = F_H(T, B). \tag{2}$$

Since the characteristic energy of the low-temperature mixed-valence state of $YbInCu_4$ is very high ($T_0 \sim 500$ K), we can assume after the authors of [25, 31] that the free energy of the mixed-valence state does not depend on temperature and magnetic field: $F_L(T, B) =$ constant. The constant value can be determined using the condition $F_L(T_v, 0) = F_H(T_v, 0)$. On the other hand, the trivalent Yb^{3+} is treated as a free ion. $F_H(T, B)$ is given by

$$F_H(T, B) = -T \ln(Q), \qquad Q = \mathrm{Tr}\left\{\exp\left(-\frac{\hat{H}}{T}\right)\right\}. \tag{3}$$

Here and below, the temperature T is expressed in units of energy. In (3) $\hat{H}$ stands for the Hamiltonian of an Yb^{3+} ion ($J = 7/2$, $g_J = 8/7$) in a cubic crystal field, which is written in terms of operator equivalents [22, 32]:

$$\hat{H} = B_0 + B_{40}(O_4^0 + 5O_4^4) + B_{60}(O_6^0 - 21O_6^4) - \vec{B}\vec{M}, \tag{4}$$

where the magnetization is given by

$$\vec{M} = \frac{g_J \mu_B}{Q} \mathrm{Tr}\left\{\vec{J} \exp\left(-\frac{\hat{H}}{T}\right)\right\}. \tag{5}$$

According to the inelastic neutron scattering study [23], in the high-temperature phase $T > 45$ K the excited Γ_6 and Γ_7 states are located at $E_6 = 3.2$ meV and $E_7 = 3.8$ meV respectively above the ground state quartet Γ_8 (we assume $E_8 = 0$). Using these values, the crystal-electric-field parameters B_0, B_{40} and B_{60} are expressed as

$$B_0 = \frac{E_6 + E_7}{4}, \qquad B_{40} = \frac{7E_6 - 9E_7}{15\,840}, \qquad B_{60} = \frac{-5E_6 - 3E_7}{332\,640}. \tag{6}$$

We calculated the magnetic phase diagram in the B–T plane using a standard procedure of diagonalization of the Hamiltonian. The results are shown in figure 6. The phase boundary lines for the three principal directions of the crystal coincide each other at high temperatures ($T > 0.8T_v$), but they are clearly separated at low temperatures. The calculated results give the largest critical field for the [110] axis and the smallest field for the [100] axis, in agreement with the experimental results (figure 2). Moreover, the calculated values of B_v are very close to the experimental ones (see table 1), although no fitting parameters were used in the calculation.

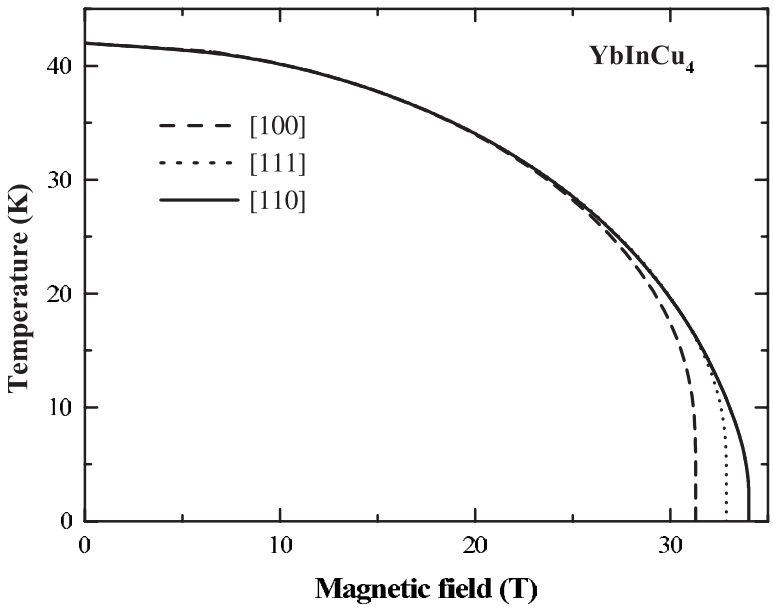

Figure 6. The calculated magnetic phase diagram of $YbInCu_4$ in the B–T plane.

This indicates that the simple free Yb ion approach developed by Dzero *et al* [25, 31] describes well the anisotropic behaviour of the field-induced transition in $YbInCu_4$.

However, it should be noted that the magnetic phase diagram reported in [25] differs from that given in the present paper, although the starting formulae are exactly the same. The wrong results given by [25] are caused by some technical errors appearing in the process of calculation.

Figure 7 shows the magnetization curves of the trivalent state calculated at 8 K by taking into account the crystal-field effects. In magnetic fields around 40 T, the magnetization is largest for the [100] axis and smallest for the [110] axis, in agreement with the experimental magnetization curves above the critical field (figure 2). The calculated magnetization is higher by about 15% than the experimental one. The possible reasons for the difference have already been discussed above. However, the order of the magnetization values calculated for the different directions is consistent with that determined experimentally (see table 1). The difference between the magnetizations of the trivalent state calculated for the [110] and [111] directions becomes very small in the low-field region below 10 T. This corresponds to the magnetization curves of $Yb_{0.8}Y_{0.2}InCu_4$ measured at a high pressure of 1.2 GPa (figure 4(b)). However, the experimental value of the magnetization measured for the [111] direction becomes largest below 3 T. (The direction of easy magnetization above 5 T is the [100] axis.) This cannot be explained by the present theoretical model. It should be noted that the $Yb_{0.8}Y_{0.2}InCu_4$ compound for 0.6 K exhibits an anisotropic ferromagnetic ordering (figure 5(a)). The magnetization in the low-field region is enhanced especially for the [111] direction; this is accompanied by the ferromagnetic ordering produced under high pressure. Perhaps the anisotropic mixing between the ground Γ_8 state and the conduction electron state will determine the anisotropy of the ferromagnetic ordering and the low-temperature susceptibility.

As described above, the magnetic anisotropy observed in the trivalent state and the phase diagram can be explained very well by the crystal-electric-field calculation on the assumption

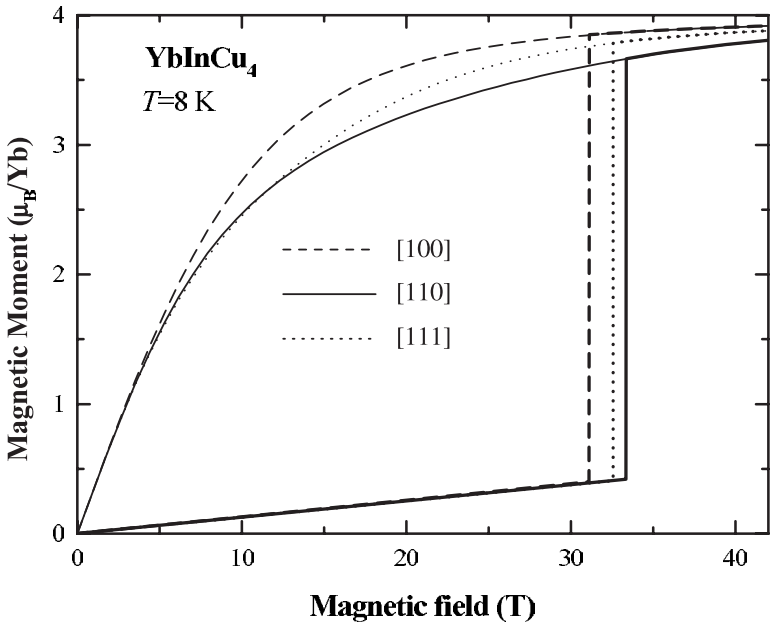

Figure 7. Calculated magnetization curves of $YbInCu_4$ at 8 K for different directions. The vertical lines correspond to the calculated critical field of the valence transition. In the low-field region, the mixed-valence state with low susceptibility is realized. The magnetization curves are depicted tentatively by thick straight lines with a small slope. (The magnetization curves in the trivalent state are shown with fine lines.) In the high-field region, the trivalent state is induced. The magnetization curves of the state are shown by thick lines.

that the free energy of the low-temperature phase is a constant. This indicates that the anisotropy in the trivalent state is caused by the interaction between the Yb 4f electrons and the crystal electric field. The same type of anisotropy is observed in the low-temperature susceptibility of $YbInCu_4$ (figure 1), in which a coherent Kondo state is formed. Maekawa *et al* [20] studied the crystal-field effects in the Kondo state in cubic crystals. It was shown that the exchange interaction between 4f and conduction electrons is strongly renormalized at low temperatures. The renormalization of the exchange interaction causes an anomalous shift and damping of the crystal-field levels. Since the crystal electric field determines the anisotropy of the magnetic susceptibility, the anisotropy may be depressed by the Kondo effect. However, we can clearly find a difference in susceptibility between different directions in the mixed-valence state (figure 1). Perhaps the crystal-field effect is non-negligible in the mixed-valence state, since the valence of Yb is still not far from 3+. Moreover, the crystal field may result in the occurrence of anisotropic coupling between conduction and 4f electrons [24], which causes anisotropy of the susceptibility.

5. Conclusions

In summary, we have measured the magnetic susceptibility and the high-field magnetization curve of single-crystalline $Yb_{1-x}Y_xInCu_4$ with $x = 0$, 0.2 and 0.3 along the principal crystallographic directions of the cubic lattice at ambient and high pressures. $YbInCu_4$ and $Yb_{0.8}Y_{0.2}InCu_4$ exhibit temperature- and field-induced valence transitions. We have found appreciable anisotropy in the susceptibility, high-field magnetization, effective moment, paramagnetic Curie temperature and critical field of the valence transition. We have calculated

the magnetization curve and the magnetic phase diagram in the B–T plane using the model of a phase transition between the free Yb^{3+} paramagnetic state in a cubic crystal electric field and the low-temperature state with constant free energy. The calculated results agree well with the experimental data of the susceptibility and high-field magnetization in the trivalent state and with the phase diagram. Moreover, we have measured the low-temperature magnetization process for $Yb_{0.8}Y_{0.2}InCu_4$ and $Yb_{0.7}Y_{0.3}InCu_4$ in low fields under high pressure and observed anisotropic ferromagnetic ordering.

Acknowledgment

This work was supported by a Grant-in-Aid for Scientific Research on Priority Areas (B) from the Ministry of Education, Culture, Sports, Science and Technology of Japan. The stay of NVM at ISSP was also supported by this Ministry.

References

[1] Bauer E 1991 *Adv. Phys.* **40** 417
[2] Felner I and Nowik I 1986 *Phys. Rev.* B **33** 617
[3] Sarrao J L 1999 *Physica* B **259–261** 128 and references therein
[4] Felner I, Nowik I, Vaknin D, Potzel U, Mozer J, Kalvius G M, Wortmann G, Schmiester G, Hilscher G, Gratz E, Schmitzer C, Pillmayr N, Prasad K G, de Waard H and Pinto H 1987 *Phys. Rev.* B **35** 6956
[5] Kojima K, Nakai Y, Suzuki T, Asano H, Izumi F, Fujita T and Hihara T 1990 *J. Phys. Soc. Japan* **59** 792
[6] Cornelius A L, Lawrence J M, Sarrao J L, Fisk Z, Hundley M F, Kwei G H, Thompson J D, Booth C H and Bridges F 1997 *Phys. Rev.* B **56** 7993
[7] Yoshimura K, Nitta T, Mekata M, Shimizu T, Sakakibara T, Goto T and Kindo G 1988 *Phys. Rev. Lett.* **60** 851
[8] Aruga Katori H, Goto T and Yoshimura K 1994 *Physica* B **201** 159
[9] Nowik I, Felner I, Voiron J, Beille J, Najib A, du Tremdet de Lacheisserie E and Gratz G 1988 *Phys. Rev.* B **37** 5633
[10] Matsumoto T, Shimizu T, Yamada Y and Yoshimura K 1992 *J. Magn. Magn. Mater.* **104–107** 647
[11] Zhang W, Sato N, Yoshimura K, Mitsuda A, Goto T and Kosuge K 2002 *Phys. Rev.* B **66** 024112
[12] Mushnikov N V, Goto T, Ishikawa F, Zhang W, Yoshimura K and Gaviko V S 2002 *J. Alloys Compounds* **345** 20
[13] Nakamura H and Shiga M 1995 *Physica* B **206/207** 364
[14] Uchida A, Kosaka M, Mori N, Matsumoto T, Uwatoko Y, Sarrao J L and Thompson J D 2002 *Physica* B **312/313** 339
[15] Mitsuda A, Goto T, Yoshimura K, Zhang W, Sato N, Kosuge K and Wada H 2002 *Phys. Rev. Lett.* **88** 137204
[16] Goltsev A V and Bruls G 2001 *Phys. Rev.* B **63** 155109
[17] Rajan V T 1983 *Phys. Rev. Lett.* **51** 308
[18] Sarrao J L, Immer C D, Fisk Z, Booth C H, Figueroa E, Lawrence J M, Molder R, Cornelius A L, Hundley M F, Kwei G H, Thompson J D and Bridges F 1999 *Phys. Rev.* B **59** 6855
[19] Fulde P 1985 *Adv. Phys.* **34** 589
[20] Maekawa S, Takahashi S, Kashiba S and Tachiki M 1985 *J. Phys. Soc. Japan* **54** 1955
[21] Irkhin V Yu and Katsnelson M I 1999 *Phys. Rev.* B **59** 9348
[22] Lea K R, Leask M J and Wolf W P 1962 *J. Phys. Chem. Solids* **23** 1381
[23] Severing A, Gratz E, Rainford B D and Yoshimura K 1990 *Physica* B **163** 409
[24] Kim T S and Cox D L 1996 *Phys. Rev.* B **54** 6494
[25] Dzero M O 2002 *J. Phys.: Condens. Matter* **14** 631
[26] Lawrence J M, Kwei G H, Sarrao J L, Fisk Z, Mandrus D and Thompson J D 1996 *Phys. Rev.* B **54** 6011
[27] Sarrao J L, Immer C D, Benton C L, Fisk Z, Lawrence J M, Mandrus D and Thompson J D 1996 *Phys. Rev.* B **54** 12207
[28] Koyama K, Hane S, Kamishima K and Goto T 1998 *Rev. Sci. Instrum.* **69** 3009
[29] Tsujii N, He J, Yoshimura K, Kosuge K, Michor H, Kreiner K and Hilscher G 1997 *Phys. Rev.* B **55** 1032
[30] Svechkarev I V, Panfilov A S, Dolja S N, Nakamura H and Shiga M 1999 *J. Phys.: Condens. Matter* **11** 4381
[31] Dzero M O, Gorkov L P and Zvezdin A K 2000 *J. Phys.: Condens. Matter* **12** L711
[32] Al'tshuler S A and Kozyrev B M 1964 *Electron Paramagnetic Resonance* (New York: Academic) ch 3